



Application of Hybrid Laser Arc Welding for Construction of LNG Tanks Made of Thick Cryogenic 9% Ni Steel Plates

Sergej Gook¹ · Abdel-Monem El-Batahy² · Andrey Gumenyuk³ · Max Biegler¹ · Michael Rethmeier^{1,3,4}

Accepted: 11 October 2023
© The Author(s) 2023

Abstract

Hybrid laser-arc welding (HLAW) was applied for butt welding of 14.5 mm thick plates of ferritic cryogenic steel X8Ni9 containing 9% Ni, which is used for manufacturing storage and transport facilities of liquefied natural gas (LNG). The weld seam formation and the achievable metallurgical and mechanical properties of the hybrid welds were investigated experimentally for two types of filler wire, an austenitic wire dissimilar to the base metal (BM) and an experimentally produced matching ferritic wire. Safe penetration and uniform distribution of the austenitic filler metal in the narrow hybrid weld could only be achieved in the upper, arc-dominated part of the weld. The pronounced heterogeneous distribution of the austenitic filler metal in the middle part and in the root area of the weld could not ensure sufficient notched impact toughness of the weld metal (WM). As a result, a decrease in the impact energy down to 17 ± 3 J was observed, which is below the acceptance level of ≥ 34 J for cryogenic applications. In contrast, the use of a matching ferritic filler wire resulted in satisfactory impact energy of the hybrid welds of up to 134 ± 52 J at the concerned cryogenic temperature of -196 °C. The obtained results contribute to an important and remarkable conversion in automated manufacturing of LNG facilities. In other words, the results will help to develop a new laser-based welding technology, where both quality and productivity are considered.

The efficiency of the developed welding process has been demonstrated by manufacturing a prototype where a segment of the inner wall of large size LNG storage tank was constructed. In this concern, hybrid laser arc welding was conducted in both horizontal (2G) and vertical (3G) positions as a simulation to the actual onsite manufacturing. The prototype was fabricated twice where its quality was confirmed based on non-destructive and destructive examinations.

Keywords Hybrid Laser arc Welding · 9% Ni Steel · Fusion zone size · Microstructure · Tensile Strength · Impact Absorbed Energy · Microstructure · Hardness

Extended author information available on the last page of the article

Introduction

Quenched and tempered 9% Ni steel is preferably supplied as X8Ni9+QT according to DIN EN 10028-4 or ASTM/ASME A553 Type 1. Due to its favorable combination of production costs and high mechanical-technological properties [1–3], X8Ni9+QT steel is best suited for use in cryogenic environments down to $-196\text{ }^{\circ}\text{C}$, where high impact strength is primarily required. The high cold resistance of this ferrite steel alloyed with nickel is comparable to that of austenitic steels and is achieved in the course of heat treatment and due to complex microstructure, which includes fine tempered-martensite with up to approx. 10% of the thermally stable retained austenite [4–6].

The large volume LNG storage tanks and containers as well as components of modern LNG fueled ships exhibit representative examples for the use of 9% Ni steel [7–9]. The LNG market continues to grow and, according to a forecast by the International Energy Agency (IEA), the global demand for LNG volumes will increase more than double by 2040 [10]. For steelmaking, this means that more and more sheets made of 9% Ni steel are needed to expand the LNG infrastructure. From the LNG plant manufacturer's side, this large tonnage of sheet metal needs to be processed by welding into a finished product. In modern LNG facilities, steel sheets made of 9% Ni steel with a thickness in the range between approx. 10 and 60 mm are used for the construction of the inner wall as well as flat bottom, which withstand the cryogenic medium [11, 12]. The design of the large above-ground LNG tanks often requires that the dome roof is also made of 9% Ni steel [13]. In LNG tank construction, the steel plates are usually welded together in multi-run technique using conventional arc welding methods. These are submerged arc welding (SAW), gas metal arc welding (GMAW), shielded metal arc welding (SMAW) or gas tungsten arc welding (GTAW). Welding can be performed in different positions. A novel vertical SAW process has been developed for this purpose [14]. It uses a small-diameter filler wire and a waving technique to control the weld pool. This results in a relatively low deposition rate of less than 100 g/min, which does not appear to be particularly effective in LNG production.

A major problem that frequently occurs with nickel alloyed steels is the residual magnetism that causes arc blow. This is a particular problem with 9% Ni steel, which can be easily and very strongly magnetized, making it impossible to perform the weld [15]. The alternating welding current (AC) is therefore recommended to prevent the arc blow effect. Other welding techniques such as friction stir welding (FSW) or electron beam welding (EBW) for joining thick sheets of 9% Ni steel are currently being researched [16, 17]. Nevertheless, according to current regulations in the LNG sector, only arc-based welding processes are used for the construction of LNG facilities.

Austenitic Cr-Ni and Ni-based filler metals are the standard welding consumables for joining 9% Ni steel as this ensures good fatigue crack resistance and high fracture toughness of welds at low temperatures [18, 19]. The regulations of the International Classification Society Det Norske Veritas and Germanischer Lloyd (DNV GL) set the required average energy of the Charpy V-notch impact test of 34 J for the welds on Ni-alloyed steels for LNG applications [20]. Projects carried out under the scope of German Technical Inspectorate (TÜV) sometimes specify a minimum Charpy tough-

ness of 0.40 J/mm^2 , corresponding to 32 J on a standard Charpy impact specimen [21]. Depending on the grade of 9% Ni steel used, other LNG projects have even higher requirements, with a minimum impact energy of 60 J as an acceptance criterion [22].

Satisfied notched impact strength of austenitic WM at $-196 \text{ }^\circ\text{C}$ on quenched and tempered 9% Ni base metal (BM) can be achieved if the welding procedure is carried out in compliance with the welding regulations. The welding process has to be carried out with the lowest heat input in order to control the grain size in the HAZ and the degree of mixing between the austenitic filler material and the ferritic base material, so as not to reduce the toughness of the welded joint [23, 24]. It is therefore recommended to limit the heat input during welding to about 3.5 kJ/mm for SAW and 2.5 kJ/mm for SMAW [25]. In addition to high toughness, maintaining the required tensile strength is an essential task when using austenitic filler metals. This is particularly the case for conventional Ni-based welding consumables, as the tensile strength of the austenitic WM is lower than that of the quenched and tempered 9% Ni steel [26]. To balance this effect, the wall thicknesses should be over-designed in order to ensure the strength of the welded construction. As a consequence, there is a greater need for materials, higher processing costs and additional construction costs, e.g. for stronger foundations.

Another factor that increases the construction costs of LNG tanks is a large amount of expensive austenitic welding consumables, which are needed to fill the edge preparations on thick plates. A more suitable approach for joining 9% Ni sheets would be the use of less expensive ferritic welding consumables of the same type as the BM. Such fillers could offer matching properties of the WM and BM as well as 100% efficiency of the weld joint. Intensive research into the development of ferritic filler materials for welding the 9% Ni-alloy was already conducted in the 1980s [27]. The latest studies show that with the use of matching ferritic filler materials and appropriate post weld heat treatment (PWHT), the required mechanical properties of cryogenic 9% Ni steel sheets can be achieved with confidence [28, 29].

Despite the existing recipes for the manufacture of ferritic consumables for cryogenic service, the use of these materials has only become established in practice for specific applications. In addition, the market availability of these fillers is still very limited. The reason for this is considered to be a possible impairment of the weld quality at operating temperature. The question of whether these filler metals represent an alternative to austenitic filler metals has not yet been clarified. Given the current state of the art, the implementation of highly efficient welding processes such as HLAW appears to be very relevant to the LNG sector, not only from an economic point of view, but also in terms of productivity and quality. The great economic potential of the HLAW process compared to the conventional welding processes results from the significant advantages of this technology, such as the high achievable penetration depth, high welding speed, low heat input during welding and ability to automate the process [30, 31]. In particular, when welding thick-walled LNG constructions, the advantages of the hybrid welding process becomes noticeable. The thick-walled parts can be welded faster and with less amount of filler material. Numerous studies showed the applicability of HLAW for single-pass welding of flat steel plates up to thicknesses of 25 mm [32–34]. An electromagnetic weld pool support allows

steel plates with a thickness of 28 mm to be joined in single layer in butt joint using the HLAW process [35]. 45 mm thick high strength steel sheets could be joined by HLAW with double-sided technique and application of metal cored wire [36]. The current state of development thus shows that existing HLAW technologies can cover the range of wall thicknesses presented in the LNG sector.

A number of studies have been carried out by research groups worldwide to investigate the application of laser-based welding techniques for joining thick plates of nickel alloyed steels [37–39]. Laser beam welding (LBW) tests have shown V-notch impact strength of up to 1.0 J/mm^2 (80 J) for 7.2 mm thick sheets of X8Ni9 [40]. The results could not be extrapolated to thicker plates. In particular, an average V-notch toughness of 0.26 J/mm^2 (21 J) was achieved for the 14.5 mm thick 9% Ni steel, which was below the acceptance level [41]. It has to be mentioned that the autogenous LBW process of 14.5 mm plate thickness was characterized by an unfavorable welding thermal cycle with a high cooling rate of up to $300 \text{ }^\circ\text{C/s}$ and no metallurgical influence on the WM was possible because no filler material was added. In [42] it is discussed that impact strength is influenced not only by the WM microstructure but also by the dimension of the heat affected zone (HAZ) and the heterogeneity of the mechanical properties, which is strongly dependent on a preheating parameter. The 14.5 mm thick plates of 9% Ni steel were preheated before LBW experiments. Preheating resulted in the formation of both WM and HAZ without significant hardness differences. Impact toughness values up to 2.28 J/mm^2 (182 J) were obtained for the preheat temperature range of 160 to $210 \text{ }^\circ\text{C}$ and cooling times $t_{8/5}$ of 2.1 and 2.3 s, respectively. The obstacle is that preheating is an additional technological step that requires special equipment and, in addition, cannot always be carried out on the construction site.

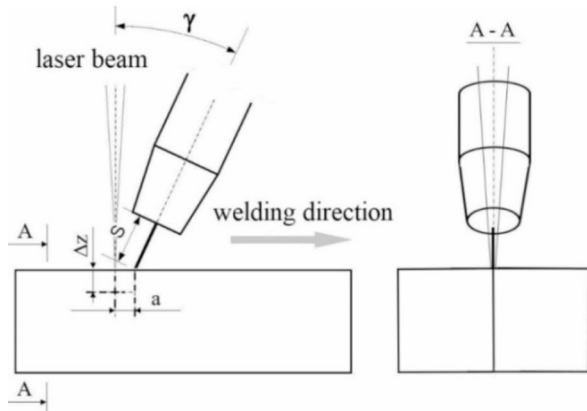
In contrast to LBW, the HLAW process offers more flexibility. Additional energy of the arc allows obtaining a more favorable welding thermal cycle. Satisfactory metallurgical or mechanical properties of the HLAW welds can be achieved by using suitable filler metals. A uniform distribution of the filler material in the narrow and deep melting zone is of importance for achieving the required mechanical properties of the hybrid welds [43–45]. Furthermore, it is of great practical interest to determine the extent to which the dilution of the filler material in the hybrid welds of cryogenic 9% Ni steels can have a positive influence on the notched impact strength of the hybrid welded joints.

The state of the art and technology shows that the application of laser-based welding technology for the LNG service is an interesting topic from an economic and technological point of view. Unfortunately, this aspect has not been sufficiently researched up to now.

This paper discusses the results of welding tests on the relationship between welding process parameters, filler wire type and achievable mechanical properties of HLAW joints of thick 9% Ni steel plates. Furthermore, attempts were made to clarify the performance of the hybrid welding process for prototype manufacturing. A segment of the inner wall of large size LNG storage tank was hybrid welded in both horizontal (2G) and vertical (3G) positions as a simulation to the actual assembly onsite.

Table 1 Chemical composition of materials, shown in wt%

Material/Element	C	Mn	Si	P	S	Cr	Nb	Ni	Mo	Cu	Fe
sheets X8Ni9+QT640	0.07	0.39	0.18	0.006	0.001	0.02		8.9	0.02	0.01	bal.
wire ERNiCrMo-3	0.03	0.2	0.25			22	3.5	bal.	9		0.97
wire ERNi11	0.013	0.4				0.045		11.3			bal.

Fig. 1 Configuration of the HLAW process

Experimental Procedure

The low carbon 9% Ni quenched and tempered steel X8Ni9+QT640 with a minimum yield strength of 640 MPa was used for the welding tests. The sheet thickness was 14.5 mm. According to the manufacturer's specifications, the steel has a tensile strength of 717 MPa and an absorbed impact energy of 197 J at a cryogenic test temperature of $-196\text{ }^{\circ}\text{C}$. The Vickers hardness is 250 HV. Austenitic solid wire ERNiCrMo-3 according to AWS A5.11 and experimentally produced ferritic wire ERNi11 with 11% Ni were selected as filler metals for comparative welding tests. The chemical compositions of the materials used are given in Table 1.

A gas mixture of Ar with 18% CO_2 as well as Ar with 30% He with a flow rate of 25 l/min served as shielding gases for HLAW tests. The back shielding was Argon 4.6 with a purity grade of at least 99.996%.

A 20 kW IPG YLR-20,000 fibre laser with an emission wavelength of 1070 nm and a beam parameter product of 11 mm x mrad was used as the laser radiation source. A HIGHYAG BIMO HP laser processing head with a focal length of 350 mm provided a focused spot diameter of the laser beam of 560 μm . The arc was powered by a Cloos Qineo Pulse 600 welding machine with a maximum current of 600 A.

The HLAW experiments were performed with an arc leading orientation where the GMAW torch was tilted at an angle (γ) of 25° to the laser beam axis. The process distance (a) between the wire tip and the laser incidence point on the workpiece surface was adjusted to 4 mm. With a negative focus position (Δz) of -3 mm, the laser beam was slightly defocused on the workpiece surface. The contact tip to work distance (S) was adjusted to 16 mm. The configuration of the HLAW process is shown schematically in Fig. 1.

The welding head was mounted on a 6-axis industrial robot. For butt welds with a technical 0-gap, sheets of 9% Ni steel with dimensions 300 mm x 200 mm x 14.5 mm were precisely aligned and clamped on the welding table. The welding setup used allowed welding in flat position 1G/PA (Fig. 2a) as well as horizontal position 2G/PC (Fig. 2b) and vertical down position 3G/PG (Fig. 2c).

After welding, the hybrid welds were visually inspected for surface irregularities in accordance with ASME IX and DIN EN ISO 13919-1 qualification standards. Selected welds were radiographed (X-rayed) in accordance with DIN EN ISO 17636-1 for internal quality assessment. Metallographic examinations and hardness measurements were carried out in accordance with DIN EN ISO 17,639 and DIN EN ISO 6507-1 respectively.

Cross sections were obtained at the middle part of welded specimens. After metallographic polishing, the samples were etched in Nital reagent (Alcoholic nitric acid 4%). The macro morphology of the welds was then examined using a Zeiss Stemi 508 stereo microscope. The microstructure of the HAZ and the WM of the welded specimens was investigated by optical microscope Zeiss Imager A1m. The X-ray diffractometry (XRD) was used for quantification of residual austenite in the WM of hybrid welds.

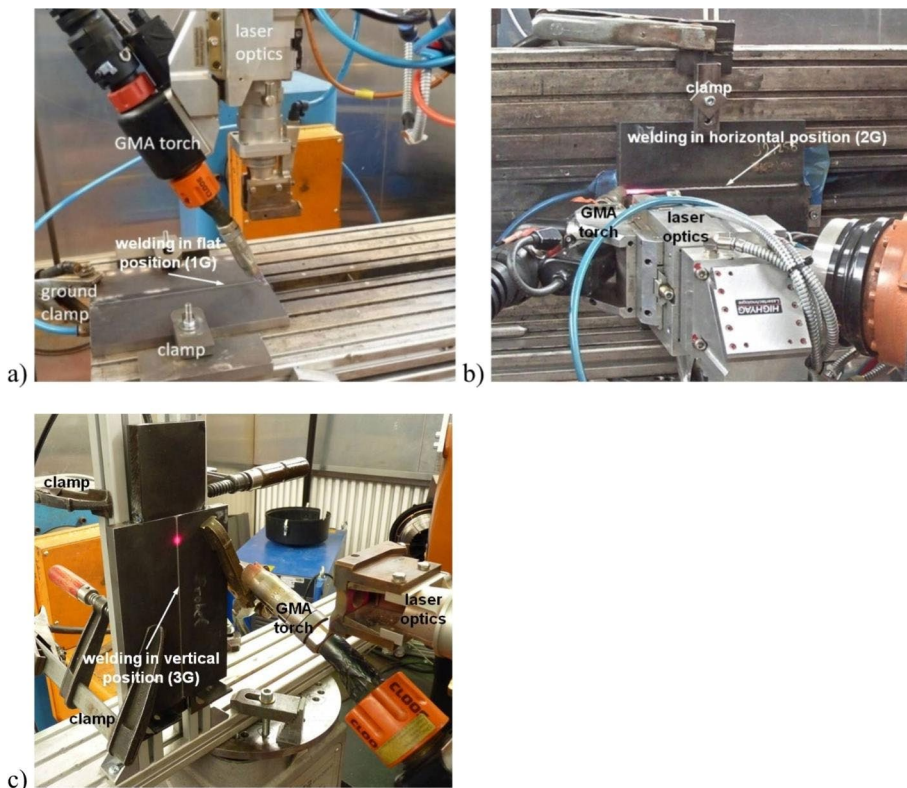


Fig. 2 Hybrid laser-GMA welding setup: laser head and GMAW torch mounted on a robot arm for welding in (a) flat position 1G, (b) horizontal position 2G and (c) vertical down position 3G

Tensile and impact tests of welded joints were carried out at room temperature and $-196\text{ }^{\circ}\text{C}$, respectively according to concerned standards. The Charpy V-notch impact test was done according DIN EN ISO 50125. The V-notch impact test specimens were processed into size of $10\times 10\times 55\text{ mm}^3$ with a 2 mm depth V-type 45° notch based on ISO 148-1. The V-notch was milled in the centerline of the laser-hybrid WM. The fracture surface morphology was characterized using a Phenom XL desktop scanning electron microscope (SEM).

Finally, a prototype was constructed where a segment of the inner wall of large size LNG storage tank was hybrid welded in both horizontal (2G) and vertical (3G) positions as a simulation to the onsite manufacturing. The prototype was constructed twice where its quality was confirmed using non-destructive and destructive examinations.

Results

External and Internal Quality of Hybrid Welds

The complete penetrated HLAW with a well-formed shape without undercuts could be produced with a laser power (P_l) of 17 kW, an average arc power (P_a) of 10 kW and welding speed (v_w) in the range between 2.5 m/min to 3 m/min. The higher welding speed in the range between 2.8 m/min and 3 m/min was preferable when using the austenitic filler metal ERNiCrMo-3. In particular, the formation of metal droplets on the root side, whose formation is favored at the low welding speed in combination with the low viscosity of the Ni melt [46], was effectively prevented. On the other hand, the applying of the ferritic 11% Ni filler wire allowed producing sound welds in a relatively wide parameter window. The higher viscosity of the Fe-Ni melt compared to the Ni-based melt meant that the molten metal was less fluid. As a result, the welding process could be carried out at the lower welding speed of 2.5 m/min without the liquid metal accumulating in the form of root droplets. The wire feeding speed (v_{wire}) could be varied in a quite wide range between 8 m/min to 18 m/min without loss in the process stability. Such possibility of varying the wire feeding speed is important for welding in different positions such as 2G (horizontal) and 3G (vertical-down) because the weld pool volume can be controlled to prevent the drop out of the melt. The process parameters used in the welding experiments and the heat input values (E_{HLAW}) are summarized in Table 2. When calculating the E_{HLAW} , a thermal efficiency of 0.8 was considered for both GMAW and laser welding [47, 48].

The results show that the HLAW process can be performed with both tested filler metals within a relatively wide parameter window. For comparison purposes, this study considered welds made with the following parameter sets:

Table 2 Range of welding parameters for single-pass HLAW of 14.5 mm thick plates X8Ni9

Filler material	P_l in kW	v_w in m/min	v_{wire} in m/min	U in V	I in A	E_{HLAW} in kJ/mm
ERNiCrMo-3, $\varnothing 1.2\text{ mm}$	17–18	2.8–3	11–14	30–33	330–350	0.43–0.5
ERNi11, $\varnothing 1.0\text{ mm}$	16–17	2.5–2.8	8–18	28–32	275–315	0.41–0.52

- filler wire ERNiCrMo-3, $P_1 = 17$ kW, $P_a = 11$ kW, $v = 2.7$ m/min, $E_{HLAW} = 0.5$ kJ/mm;

- filler wire ERNi11, $P_1 = 17$ kW, $P_a = 9$ kW, $v = 2.5$ m/min, $E_{HLAW} = 0.5$ kJ/mm.

Figure 3 shows typical external appearances of HLAW joints for both the austenitic filler wire ERNiCrMo-3 and the ferritic filler wire containing 11% Ni. A well-formed weld top surface as well as uniform root could be reproduced for both filler wires tested in a series of welds. The X-ray images in Fig. 4 show that there are no cracks or pores in the welds. The evaluation of the external as well as internal quality allows the hybrid welds to be assigned to the highest evaluation class B according to DIN EN ISO 13919-1. The end crater was not optimized, therefore it is not considered in the quality evaluation.

Macro- and Microstructural Characteristics of Hybrid Welds

Figure 5 shows macrographs of hybrid welds made using both austenitic wire and ferritic wire, as well as light optical micrographs for different parts of the weld.

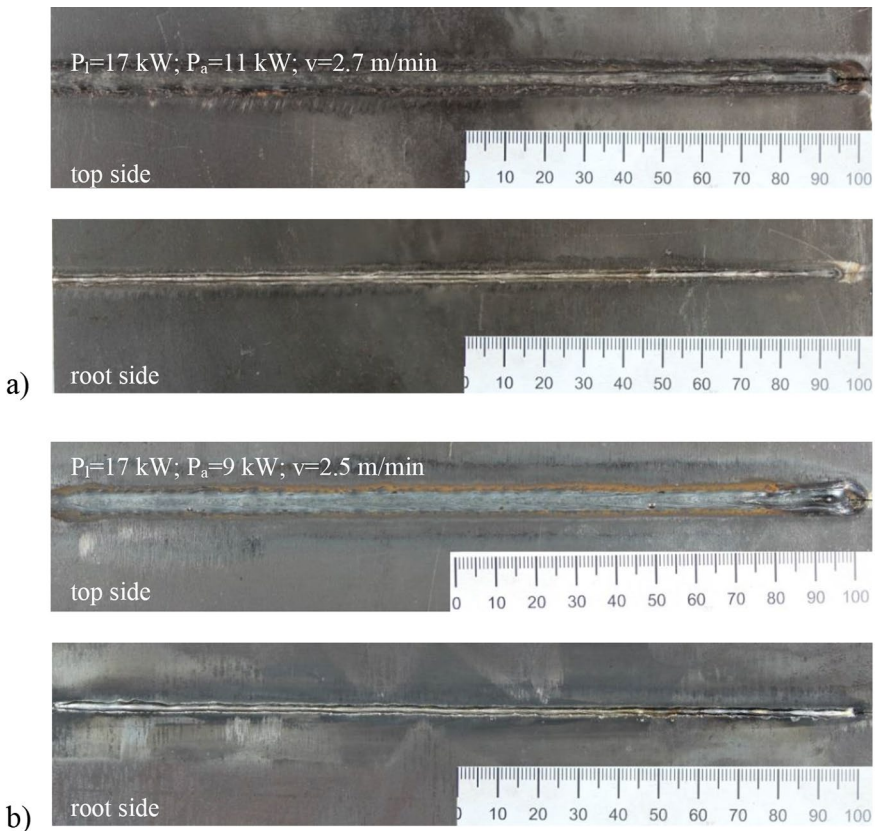


Fig. 3 Outer appearances of the HLAW joints produced on 14.5 mm thick sheets X8Ni9 using (a) ERNiCrMo-3 austenitic filler metal and (b) ferritic filler wire containing 11% Ni

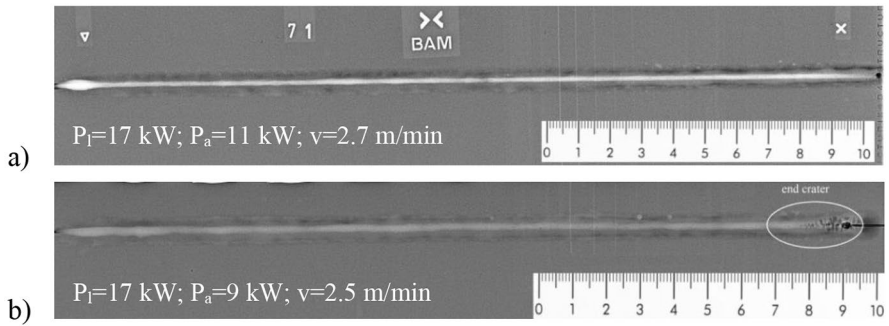


Fig. 4 X-ray pictures of the HLAW joints produced on 14.5 mm thick plates X8Ni9 using (a) ERNiCrMo-3 austenitic filler metal and (b) ferritic filler wire containing 11% Ni

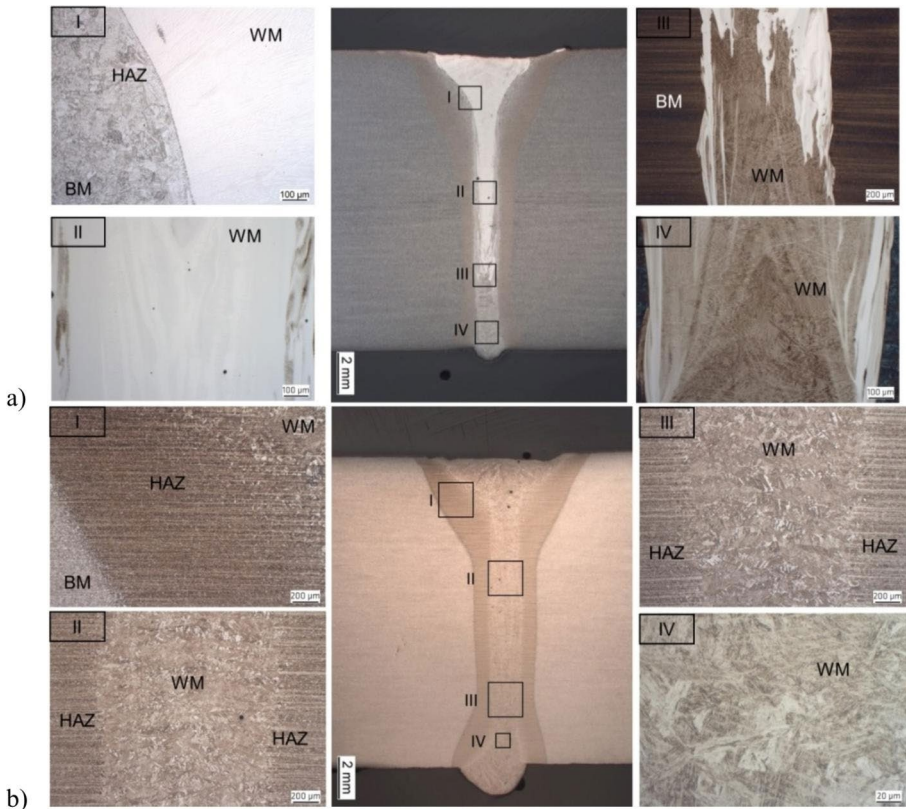


Fig. 5 Cross sections of hybrid welds produced using (a) austenitic wire ERNiCrMo-3 and (b) ferritic wire with 11% Ni

The macro sections allow the quality of hybrid welds to be evaluated. Unacceptable internal imperfections such as lack of fusion or cracks were not found. However, some pores with a maximum pore diameter of 30 μm could be detected. Such defects are subcritical and will pass the welding code requirements in LNG sector.

Despite the fact that the HLAW welds do not show any significant irregularities, some differences in the microstructure can be observed already at the macroscopic level. While the upper, arc dominated part of the weld in Fig. 5a has a predominantly austenitic microstructure due to Ni-based filler wire, a heterogeneous mix of austenitic filler and martensitic BM could be observed in the middle part of the weld. There are pronounced Ni-rich mixing areas, shown as white areas in the cross sections. The penetration pattern of the austenitic filler becomes narrow and stops abruptly at around 2/3 of the sheet thickness. The light microscopic examination shows that only a small amount of austenitic filler metal reaches the root of the weld. Martensitic microstructure with some traces of austenite predominates in the root area.

The weld in Fig. 5b, on the other hand, shows no macrostructural changes over the weld thickness. The 11% Ni filler is chemically similar to BM and promotes the formation of a homogeneous microstructure consisting of fine martensite with large amounts of blocks and packets nucleated at the boundaries of the prior austenite grains. Such a “block-and-packet” structure indicates structural modifications of martensite such as lath martensite, which is predominantly found in unalloyed and low-alloy steels with less than 0.4% C, but also in 9% Ni steel [49].

It is of great practical interest to determine the extent to which the dilution of the filler metal in the HLAW of cryogenic 9% Ni steel can positively influence notched impact toughness of the welded joints. EDX analysis was carried out to quantify the distribution of the filler wire in the weld cross section. The element Ni was chosen as the contrast element and its concentration was analyzed in three planes in the cross section of the hybrid welds for both the austenitic and ferritic filler wires (Fig. 6). The nominal Ni content of ERNiCrMo-3 wire is approximately 61% by weight (Table 1). In hybrid welds made with ERNiCrMo-3 austenitic wire, an average Ni concentration of 25% was measured at the weld neck. The maximum Ni content in the middle part of the weld also reached 25%, although the width of the Ni enriched region decreased significantly. The average Ni content in the root part of the weld was slightly over 10% (Fig. 6a). Thus, the EDX measurements show a drastic reduction of the Ni concentration through the weld seam thickness. The average Ni content within the weld produced with ferritic 11% Ni wire (Fig. 6b) is slightly above 10% in the top part of the weld. The average Ni content is 9.5% in the center of the weld and 9% in the root area, indicating a fairly even distribution of Ni across the weld cross section.

The EDX measurements in Fig. 6 reveal a good correlation with the light microscopical observations of the flow patterns in Fig. 5.

The good low-temperature toughness of 9% Ni steel is assumed to be due to stable retained austenite phases in an otherwise tempered martensitic matrix [50]. In this work, the amount of retained austenite was determined using an X-ray diffractometer with Cr $K\alpha$ radiation, powered at a voltage of 30 kV and a current of 40 mA. The X-ray diffractometer was operated at the θ -2 θ (Bragg-Brentano) mode. The quantitative characterization was made on the ground of the proportion of the diffraction maximum integral intensity of plane system (111): austenite ($2\theta=67.1^\circ$) and (110)

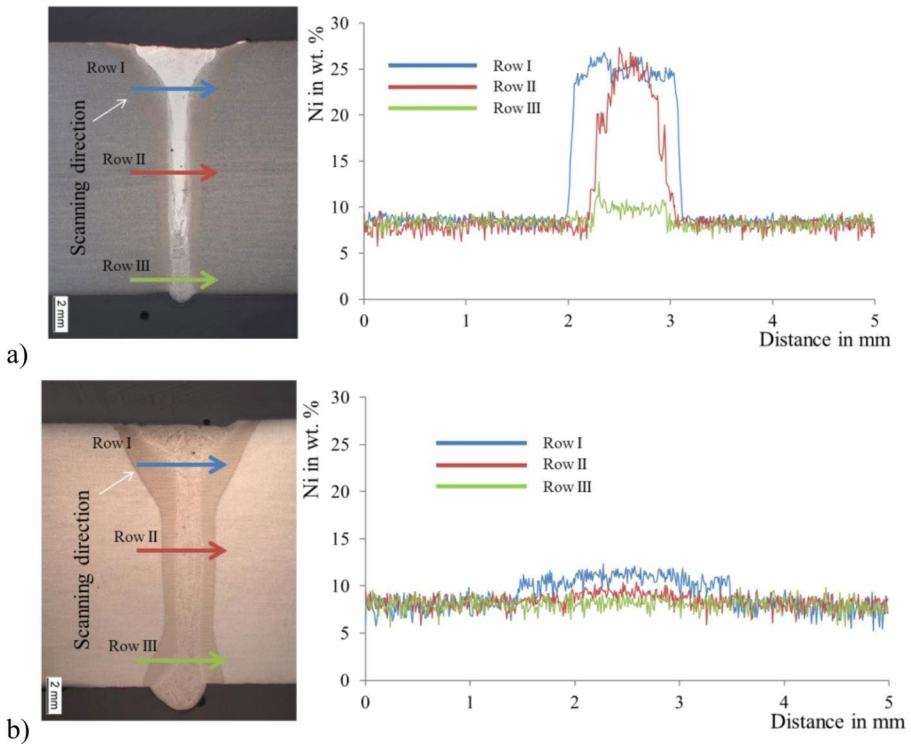


Fig. 6 EDX results of the Ni distribution in three planes **(a)** of the HLAW with austenitic filler wire ERNiCrMo-3 and **(b)** of the HLAW with ferritic 11% Ni filler wire

martensite ($2\theta=68.7^\circ$) phase. The XRD measurements were performed both for austenitic and ferritic filler metal. The measurement points, one millimeter in diameter, were placed in two regions of the weld: weld neck and weld root. Figure 7 shows the XRD patterns for the samples analyzed in the present work. The peaks detected could only be attributed to martensite and austenite. There were no significant peaks of carbides or precipitates among the diffraction peaks.

It is worth noting that in the upper part of the weld made with ERNiCrMo-3 austenitic welding wire there is an increased content of retained austenite of 86% (Fig. 7a). In the root region of this weld, the retained austenite content does not exceed 3.5% (Fig. 7b). The distribution of retained austenite thus correlates with the dilution pattern of the austenitic filler wire across the weld thickness. For the weld made with 11% Ni ferritic wire, no variations in Ni content were found across the weld cross section. The Ni content is approximately 3.5% for both measurement points (Fig. 7c and d).

Mechanical Testing of Hybrid Welds

Hardness distribution across the weld is closely related to other mechanical properties of the joint such as tensile strength and impact toughness. In this study, hardness

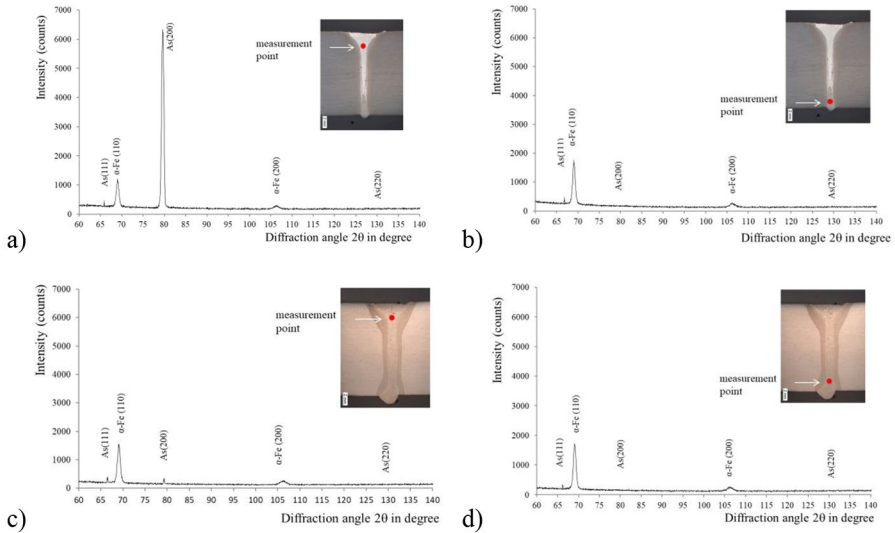


Fig. 7 XRD patterns of the weld metal for (a) the top of the weld made with austenitic ERNiCrMo-3 filler wire, (b) the root of the weld made with austenitic ERNiCrMo-3 filler wire, (c) the top of the weld made with ferritic 11% Ni filler wire, (d) the root of the weld made with ferritic 11% Ni filler wire

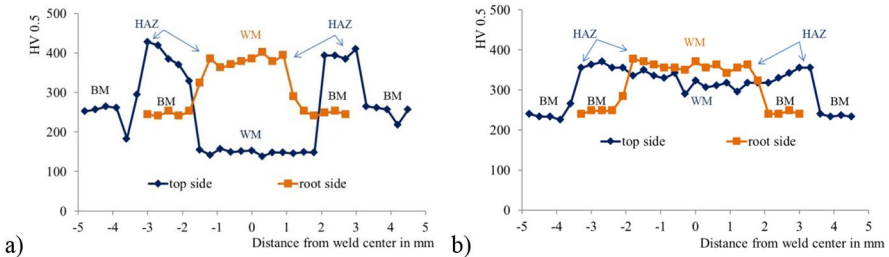


Fig. 8 The Hardness profiles of top and root sides of laser hybrid weld joints produced using (a) austenitic ERNiCrMo-3 filler wire and (b) ferritic 11% Ni filler wire

measurements were taken at the top and bottom of the weld cross sections at 5 mm distance from the weld surface. The HV0.5 hardness profiles of the top and root sides of the hybrid welds are shown in Fig. 8. In particular, Fig. 8a shows the character of the hardness distribution for the weld made using the austenitic filler wire ERNiCrMo-3. A difference between the hardness values of the top and bottom sides of the weld zone can be observed. The hardness of the top side of the weld of 151 HV0.5 is much lower than that of the root side of 385 HV0.5. This can be explained by the different chemical composition of the top and root sides of the weld zone.

The lower hardness of the weld top side is related to its higher content of Ni, which is an austenite forming element. In other words, higher amount of the ductile austenite phase in the weld top side results in lower hardness, in comparison with that of martensitic structure of the weld bottom side. The highest hardness values in the range

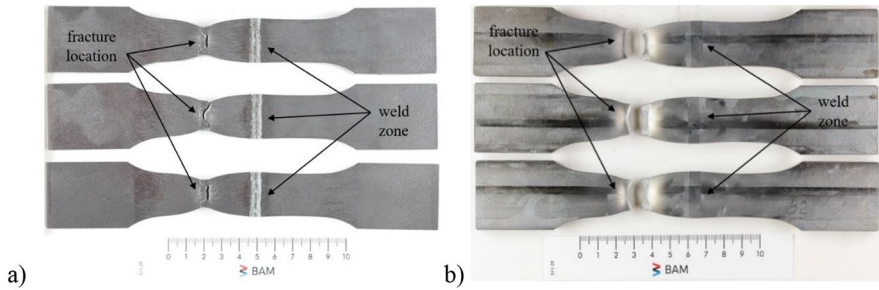


Fig. 9 Fractured tensile test specimens: (a) laser hybrid weld produced using austenitic ERNiCrMo-3 filler wire and (b) ferritic 11% Ni filler wire

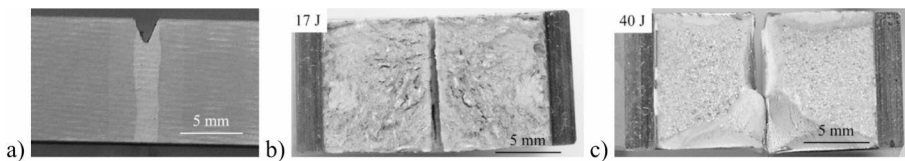


Fig. 10 Charpy V-notch specimens before and after testing: (a) location of the V-notch in the weld center, (b) macro view of the fracture surface of the weld produced using austenitic ERNiCrMo-3 filler wire and (c) ferritic 11% Ni filler wire

of 390 HV0.5 to 410 HV0.5 were obtained in the HAZ of both the top and root sides of the weld due to the hard martensitic structure formed in the HAZ.

Hardness profiles of top and root sides of laser hybrid butt weld produced using ferritic 11% Ni filler wire are shown in Fig. 8b. It can be noticed that quite wide fusion zone with a width of 7 mm was obtained. Another important notice is that no considerable difference in hardness values of both top and root sides of weld zone was observed. The average hardness value 366 HV0.5 of the weld zone top side is close to that of the root side (381 HV0.5). This is related to similar chemical compositions of both top and root sides of the weld zone. Compared to the BM hardness (252 HV0.5), HLAW with ferritic 11% Ni filler wire resulted in a hardening of the WM of approximately 50% above the BM hardness. No hardness softening effects or peaks were observed in the HAZ.

Figure 9 shows the fractured tensile test specimens of hybrid welds made using either the austenitic filler wire ERNiCrMo-3 or the ferritic filler wire ERNi11. Three specimens per material combination were tested. All specimens successfully passed the tensile test. The average ultimate stress of 720 ± 3 MPa with fracture location in the BM far from the weld zone could be reproducibly achieved.

The impact test was carried out at the test temperature of -196 °C. A set of five specimens was tested for each material combination. The higher accuracy micro-machining CNC system was used to adjust the V-notch in the center of the WM. The location of a micro machined V-notch in relation to the center of the WM is shown exemplarily in Fig. 10a. The characteristic examples of fracture surfaces for

welds produced using austenitic and ferritic filler wires are shown in Fig. 10b and c respectively.

The use of ERNiCrMo-3 austenitic filler resulted in a low V-notch impact energy below the required value of 34 J. On the other hand, the use of an 11% Ni filler wire resulted in higher impact energy values. The laser hybrid welds made with different filler metals showed different fracture behavior during the impact test. Further details of the fracture behavior of the tested welds are provided by the SEM fractography in Fig. 11.

The fracture surface morphology of the weld with austenitic filler wire in Fig. 11a, where the impact energy of 17 J was obtained, is indicative of brittle fracture. The presence of microcracks in the WM reduces the cryogenic impact toughness. The inhomogeneous mixing of austenitic filler material and ferritic BM results in areas with different physical properties, e.g. thermal expansion. This can lead to solidification cracking in this mixed WM. The microcracks are clearly visible in the SEM images in Fig. 11a. The fracture surface in Fig. 11b belongs to the weld made with ferritic filler metal and, with an impact energy value of 40 J, represents a mixture of a brittle fracture (zone II) and an intergranular fracture with ductile dimples (zones I and III).

Remarkably, when using ferritic wire, there is a correlation between impact energy and wire feed speed v_{wire} or process heat input E_{HLAW} . The highest impact energy value 134 ± 52 J could be obtained for the v_{wire} 18 m/min (E_{HLAW} 0.50 kJ/mm). The lowest impact energy of 28 ± 7 J was obtained at a relatively low v_{wire} of 8 m/min (E_{HLAW} 0.41 kJ/mm). Figure 12 summarizes the details of the material combinations tested, the welding parameters used and the impact energy values achieved.

The scatter of individual impact energy values is explained by the fracture path deviation (FPD) in bending. The minimum impact energy above the required value of 34 J was achieved for wire feed rates in the range 14 m/min to 18 m/min for the ferritic filler wire. Satisfactory impact test results could not be obtained with the austenitic filler wire and the matching ferritic filler wire at the low feed rate.

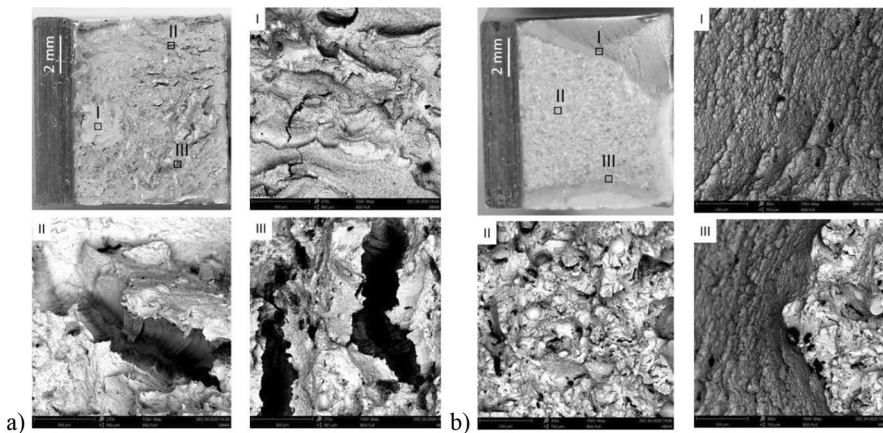


Fig. 11 SEM images taken from fractured Charpy impact specimens of (a) the weld produced using austenitic ERNiCrMo-3 filler wire and (b) ferritic 11% Ni filler wire

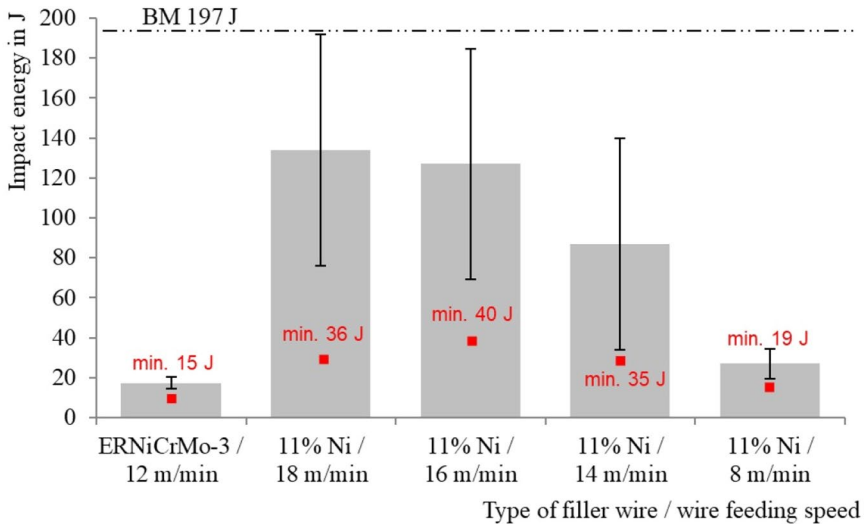


Fig. 12 Absorbed impact energy at $-196\text{ }^{\circ}\text{C}$ for the HLAW on 14.5 mm thick X8Ni9 plates

Discussion

The type of filler metal is an important factor in achieving satisfactory HLAW joints on 14.5 mm thick sheets of 9% Ni steel. The single pass HLAW process with its low heat input and high welding speed has resulted in a narrow width for both WM and HAZ, which is of remarkable importance for maintaining the mechanical properties. A stable and reproducible welding process with good weld formation was achieved in a relatively wide parameter window for both filler materials tested, the austenitic ERNiCrMo-3 filler wire and the less expensive matching ferritic 11% Ni filler wire.

In the case of the austenitic filler, a drop in the strength of the laser hybrid weld was to be expected due to the relatively soft austenitic WM indicated by the hardness measurement in Fig. 8a. Nevertheless, the tensile test showed reproducibly good results for all joints made with the austenitic filler material ENiCrMo-3. The ultimate strength achieved was equal to that of the BM and therefore met the requirements of the ASME code. In fact, the tensile specimens were fractured in the BM far from the WM and HAZ. Apparently, the local width of the undermatched austenitic WM is small compared to the plate thickness and has a negligible negative effect on the global weld strength [51].

The use of experimentally produced 11% Ni ferritic filler wire played a significant role in maintaining not only the tensile strength but also the impact toughness of the HLAW joint, despite the martensitic structure of its weld zone. This is attributed to the fact that the chemical composition of the weld zone, particularly the Ni content, is similar to that of the BM and the weld zone is relatively small. It is noteworthy that the impact energy correlates with the heat input of the welding process, which is controlled by the wire feed speed or welding current. The heat input of the HLAW process in the range 0.45 kJ/mm (v_w 14 m/min) to 0.50 kJ/mm (v_w 18 m/min) proved

to be good for maintaining sufficient impact energy. At a low wire feeding speed v_w 8 m/min, a relatively low heat input of 0.41 kJ/mm is achieved. The amount of filler material added is low and the cooling rate of the weld zone is closer to that of laser beam welding, where insufficient impact energy was found for the 14.5 mm thick X8Ni9 sheets [41].

An acceptable impact toughness of hybrid laser-arc welded joint could not be maintained using the commercially available austenitic filler wire ERNiCrMo-3 since its major volume is deposited at the weld zone top and it is difficult to be penetrated toward the weld root as a result of narrow weld root width. The ductile austenitic structure is obtained mainly at the weld top zone while less ductile structure is formed at the weld lower zone. The problem with insufficient penetration of the austenitic filler metal in the HLAW of a ferritic BM has a high potential for optimization. There is a great practical interest in carrying out the HLAW process in such a way that better mixing is achieved. The research work of Muhammad et al. [52] proves experimentally that the direction of wire feeding affects the mixing behavior. The study shows that in GMA leading configuration is an unfavorable solidification front in the weld pool present that may obstruct the circulation of the melt flow between the weld surface and root and reduce the mixing of weld metal. In the GMA trailing configuration, the flow recirculation is more pronounced and mixing is more efficient than in the GMA leading case. The study emphasizes that the absence of such recirculation in the GMA leading configuration can be seen as the main reason for having low mixing at the bottom part of the weld. This observation results in the recommendation to perform the HLAW process in a GMA trailing configuration. However, experience shows that such process configuration is only feasible up to a sheet thickness of approx. 10 mm. With higher wall thicknesses of welded parts, problems with process instabilities such as increased droplet formation will occur [53]. The use of thin nickel foil strips in the joint can promote the austenite formation in the complete cross section of the HLAW weld [54]. In [55] a TIG welding process is described in which a 0.5 mm thick Ni interlayer is introduced into the groove to improve the cryogenic toughness of the 9% Ni welded joint. Another method to realize a homogeneous distribution of the filler metal in the weld seam for thick plates is a so-called “two-step process”, in which the austenitic filler metal is applied to the edges of the weld partners by means of laser metal deposition (LMD) in the first step. In a second step, the parts coated in this way are HLAW welded [56].

Thus, it can be seen that methods for solving the problem of inhomogeneous mixing of filler metal can be proposed, although they are associated with the introduction of additional technological steps in the production procedure. The use of these techniques for welding of thick sheets X8Ni9 for LNG sector is fundamentally possible, but has not been investigated within the framework of the present study.

The results obtained indicate that the controlling factors in producing a welded joint with an acceptable combination of tensile strength and impact toughness are both the chemical composition and the size of the weld zone as a function of the filler wire and the HLAW process parameters.

All the welding experiments discussed above were carried out only in the flat welding position (1G), as shown in Fig. 2a. On the other hand, the actual on-site manufacturing of large LNG storage tanks is carried out using not only flat welding

position, but also horizontal (2G) and vertical (3G) positions [14, 57]. In this concern, the optimum welding parameters achieved for flat welding position (Fig. 2a) were properly adapted for both horizontal position (Fig. 2b) as well as vertical-down position (Fig. 2c), which in turn maintained high weld quality. While the laser power (P_L) and welding speed (v) remained constant, the wire feed speed (v_w) had to be decreased in order to reduce the molten pool volume and to prevent the molten metal from flowing out of the weld zone. Proper welding parameters for well processed single-pass HLAW of 14.5 mm thick X8Ni9 plates in different welding positions are summarized in Table 3.

Based on these proper welding parameters, successful attempts were made for prototype manufacturing where a wall segment of large size LNG storage tank was fabricated using HLAW of 14.5 mm thick cryogenic 9% Ni steel plates. Concerning this, welding was conducted in both horizontal (2G) and vertical (3G) positions as a simulation to the actual onsite manufacturing. This prototype, with an overall dimension of approximately 500 mm x 1000 mm, was twice fabricated and its quality was confirmed using non-destructive and destructive tests.

Figure 13 shows schematic illustration of LNG storage tank (a), HLAW in horizontal (2G) and vertical (3G) positions of prototype of a wall segment of LNG storage tank (b), overall view of fabricated prototype as a simulation to the onsite manufacturing (c) and macrograph of a cross section of fabricated prototype showing well processed weld bead with full penetration, narrow and sound weld confirming high quality (d). This successfully manufactured prototype is an important practical step for introducing laser-based welding technology to the LNG industry to replace the currently used conventional arc welding technology.

Conclusion

The type of filler metal as well as the applied process parameters play an important role in the HLAW of 14.5 mm thick plates of 9%Ni steel in order to obtain satisfactory welded joints.

The full penetration single pass HLAW process, with its moderate heat input and high welding speed, resulted in a narrow width for both WM and HAZ, which is of remarkable importance for maintaining the mechanical properties of the welded joints. With appropriate selection of welding parameters, a stable and reproducible HLAW process with good weld formation was achieved for both filler materials

Table 3 Proper welding parameters for well processed single-pass HLAW of 14.5 mm thick X8Ni9 plates in different welding positions

Filler Material	welding position	P_L in kW	v_w in m/min	v_{wire} in m/min	U in V	I in A	E_{HLAW} in kJ/mm
ferritic wire	flat (1G)	17	2.5	18	32	315	0.52
ERNi11, Ø1.0 mm	horizontal (2G)	17	2.5	14	31	300	0.50
	vertical down (3G)	17	2.5	10	30	285	0.49

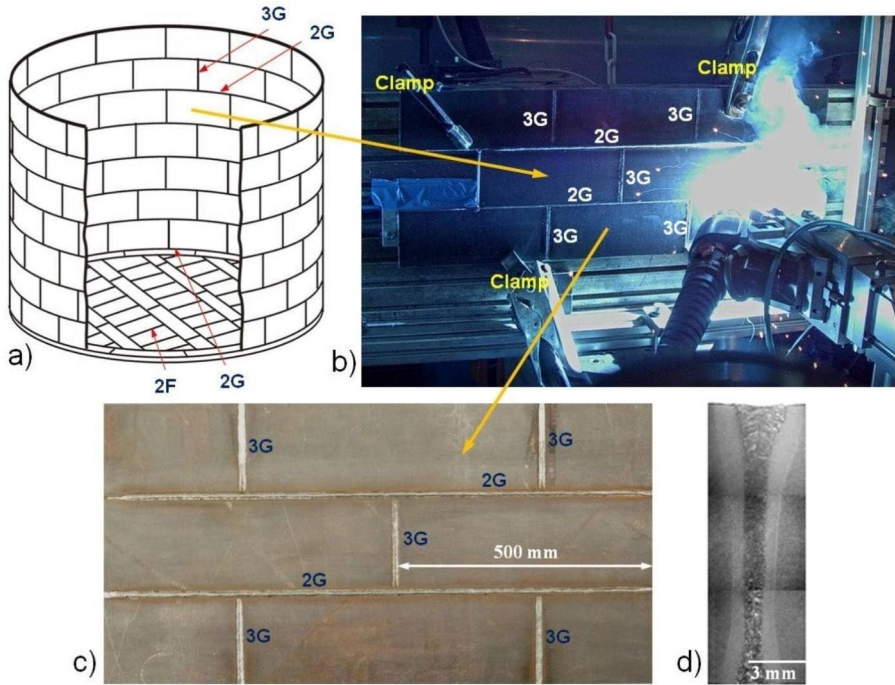


Fig. 13 Schematic illustration of LNG storage tank (a), HLAW in horizontal (2G) and vertical (3G) positions of prototype of a wall segment of LNG storage tank (b), overall view of fabricated prototype as a simulation to the onsite manufacturing (c) and macrograph of a cross section of fabricated prototype showing well processed weld bead with full penetration, narrow and sound weld confirming its high quality (d)

tested, the austenitic filler wire ERNiCrMo-3 and the experimentally produced ferritic filler wire ERNi11 with 11% Ni.

The satisfactory tensile properties of the hybrid welds were obtained for both the austenitic filler wire ERNiCrMo-3 and the experimentally produced ferritic filler wire ERNi11. The local width of the undermatched austenitic WM is small compared to the plate thickness and has a negligible negative effect on the global weld strength. All tensile specimens tested fractured in the BM far from the WM and HAZ.

While the use of the ferritic filler wire ERNi11 resulted in satisfactory impact energy values, the austenitic filler wire ERNiCrMo-3 did not result in acceptable impact toughness at the test temperature of $-196\text{ }^{\circ}\text{C}$. This is due to the fact that most of the austenitic filler material was deposited at the top of the weld zone without reliable penetration to the root of the weld. Additional technological steps are required to achieve uniform distribution of the austenitic filler material in the narrow laser hybrid weld.

The results obtained indicate that the controlling factors in producing a welded joint with an acceptable combination of tensile and impact strength are both the chemical composition and the size of the weld zone as a function of the filler wire and the HLAW process parameters.

The efficiency of the HLAW process for the LNG industry has been successfully demonstrated by a prototype construction where a segment of the inner wall of large size LNG storage tank was successfully fabricated. Concerning this, HLAW was performed in both horizontal (2G) and vertical (3G) positions simulating the actual production conditions for the construction site. This is of remarkable importance for introducing HLAW technology to the LNG industry for possible replacing the currently implemented conventional arc welding technology.

Acknowledgements The authors would like to thank Voestalpine Böhler Welding, Germany GmbH for supplying the welding consumables and Mr. Grunwald from the Division 8.3 (Radiological Methods) of the BAM for the X-ray images. Thanks are also extended to PETROJET-Egypt for the technical advice during the prototype construction.

Author Contributions A.E. and A.G. developed the theoretical framework; S.G. and A.E. performed the experiments and collected and analysed the data; M.B. aided in interpreting the results and worked on the manuscript. S.G. and A.E. wrote the main text of the manuscript; M.R. contributed to designing and conducting the study, analysing the results and drafting the manuscript.

Funding The research work was carried out within the joint innovative project (GERF ID5111-Egypt and 01DH14012-Germany) between Central Metallurgical Research and Development Institute (CMRDI) of Egypt and Fraunhofer IPK of Germany. The project was supported by the Science and Technology Development Fund (STDF) of the Arab Republic of Egypt and the Federal Ministry of Education and Research (BMBF) of the Federal Republic of Germany.

Open Access funding enabled and organized by Projekt DEAL.

Data Availability Not applicable.

Declarations

Competing Interests The authors declare no competing interests.

Ethical Approval Not applicable.

Open Access This article is licensed under a Creative Commons Attribution 4.0 International License, which permits use, sharing, adaptation, distribution and reproduction in any medium or format, as long as you give appropriate credit to the original author(s) and the source, provide a link to the Creative Commons licence, and indicate if changes were made. The images or other third party material in this article are included in the article's Creative Commons licence, unless indicated otherwise in a credit line to the material. If material is not included in the article's Creative Commons licence and your intended use is not permitted by statutory regulation or exceeds the permitted use, you will need to obtain permission directly from the copyright holder. To view a copy of this licence, visit <http://creativecommons.org/licenses/by/4.0/>.

References

1. Hoshino, M., Saitoh, N., Muraoka, H., Saeki, O.: Development of super-9% ni steel plates with superior low-temperature toughness for LNG storage tanks. *Shinmittetsu Giho*, 17–20. (2004)
2. Kern, A., Schriever, U., Stumpfe, J.: Development of 9% nickel steel for LNG applications. *Steel Res. Int.* **78**(3), 189–194 (2007)

3. Yoon, Y.K., Kim, J.H., Shim, K.T., Kim, Y.K.: Mechanical characteristics of 9% Ni steel welded joint for LNG storage tank at cryogenic. In *International Journal of Modern Physics: Conference Series* (Vol. 6, pp. 355–360). World Scientific Publishing Company. (2012)
4. Fultz, B., Kim, J.I., Kim, Y.H., Kim, H.J., Fior, G.O., Morris, J.W.: The stability of precipitated austenite and the toughness of 9Ni steel. *Metall. Trans. A*. **16**(12), 2237–2249 (1985)
5. Zhang, J.M., Li, H., Yang, F., Chi, Q., Ji, L.K., Feng, Y.R.: Effect of heat treatment process on Mechanical properties and microstructure of a 9% Ni Steel for large LNG Storage tanks. *J. Mater. Eng. Perform.* **22**(12), 3867–3871 (2013)
6. Poletskov, P.P., Nikitenko, O.A., Chukin, D.M., Gushchina, M.S., Fedoseev, S.A.: On microstructure formation features of 9% nickel cold-resistant steel and its properties brought about by different heating treatment procedures. *J. Chem. Technol. Metall.*, **53**(5). (2018)
7. Thierçault, J., Egels, C.: Cryogenic above ground storage tanks: Full containment and membrane comparison of technologies. In *LNG 17 International Conference & Exhibition on Liquefied Natural Gas* (pp. 1–8). (2013)
8. Yang, Y.M., Kim, J.H., Seo, H.S., Lee, K., Yoon, I.S.: Development of the world's largest above-ground full containment LNG storage tank. In *23rd World Gas Conference, Amsterdam* (pp. 1–14). (2006), June
9. Kim, B.E., Park, J.Y., Lee, J.S., Kim, M.H.: Study on the initial design of an LNG fuel tank using 9 wt.% nickel steel for ships and performance evaluation of the welded joint. *J. Weld. Join.* **37**, 555–563 (2019)
10. Cronshaw, I.: World Energy Outlook 2014 projections to 2040: Natural gas and coal trade, and the role of China. *Australian J. Agricultural Resource Econ.* **59**(4), 571–585 (2015)
11. Toussaint, P., Pillot, S., Chauvy, C.: Challenges, Properties, and Features of 9% Nickel Steel Plates for LNG Storage and Transport: Towards Ultra-Large Designs. In *15th International Conference and Exhibition on Liquefied Natural Gas (LNG 15)*, Barcelona, Spain. (2007)
12. Kubo, T., Ohmori, A., Tanigawa, O.: Properties of High Toughness 9% Ni Heavy Section Steel Plate and Its Applicability to 200 000 kl LNG Storage Tanks. *KAWASAKI STEEL TECHNICAL REPORT-ENGLISH EDITION-*, 72–79. (1999)
13. Ogawa, Y., Sakamoto, M., ToyOMASU, K., Ohyama, M., Fukagawa, M., Saiga, Y.: LNG Tank-its structure, the materials and welding techniques. *Tetsu-to-Hagane*. **64**(1), 135–144 (1978)
14. Sakamoto, R., Kobayashi, K., Iijima, T., Mizo, Y.: Development of submerged arc Welding Method in a Vertical Upward position. *Weld. World*. **56**(7–8), 64–71 (2012)
15. Qu, Z.X., Xia, L.Q., Wang, X.J.: The study on Welding Technology of 9Ni Steel. *Mater. Sci. Forum*. **941**, 516–523 (2018). <https://doi.org/10.4028/www.scientific.net/msf.941.516>
16. Casanova, J., Sorger, G., Vilaça, P., Brandi, S.D.: Microstructure and mechanical properties of 9% nickel steel welded by FSW. *Int. J. Adv. Manuf. Technol.*, 1–16. (2020)
17. Kim, S.H., Kang, C.Y., Bang, K.S.: Weld metal impact toughness of electron beam welded 9% ni steel. *J. Mater. Sci.* **36**(5), 1197–1200 (2001)
18. Kobelco's Welding Consumables for LNG Storage Tanks Made of 9% Ni Steel, *KOBELCO Welding Today*, Vol. 14; No. 2. (2011)
19. Schweißtechnische: Verarbeitung Nickellegierter Stähle für Tieftemperaturanwendungen, *Merkblatt DVS 0955*
20. DNVGL Maritime: 'Rules for classification - part 2 materials and welding' (2017)
21. Holloway, G., Marshall, A.: Is Welding Stainless Steel For LNG Applications Easy? *Stainless Steel World*, 421–427
22. Strömberg, J., Pak, S.S.H.: Cost Efficient LNG Storage Tank Constructed by High Productivity Welding. *ESABPO-30*, Gothenburg
23. Huan, Y.A.N.C., L. I., W.L., Shiwu, B.A.I.: Factors influencing notch toughness of Coarse-grained heat affected Zone for 9% Ni Steel [J]. *J. Mech. Eng.*, 18. (2010)
24. Khourshid, A.E.F.M., M., Ghanem, A.: The influence of welding parameters on brittle fracture of Liquefied Natural Gas Storage Tank Welded Joint. *Mater. Sci. Appl.* **4**, 198–204 (2013)
25. Hanova, E.: MMA welding of 17 501 (9% ni) steel. *Weld. Int.* **2**(8), 755–762 (1988)
26. Ohkita, S.: Control of strength and toughness in Weld metals. *Weld. Int.* **17**(9), 693–698 (2003)
27. Mahin, K.W., Morris, J.W., Watanabe, I.: A review of the development of Ferritic Consumables for the welding of 9%-Nickel steel: Research in the United States and Japan. In: *Advances in Cryogenic Engineering Materials*, pp. 187–199. Springer, Boston, MA (1980)

28. El-Batahgy, A., Saiyah, A., Khafagi, S., Gumenyuk, A., Gook, S., Rethmeier, M.: Shielded Metal arc Welding of 9% Ni Steel Using Matching Ferritic Filler Metal, pp. 1–7. *Science and Technology of Welding and Joining* (2020)
29. Brätz, O.: Artgleiches Unterpulverschweißen Von 9%-Nickelstählen an Kryogenen LNG-Tanks für Schiffbauliche Anwendungen, DVS Congress 2019. Große Schweißtechnische Tagung, Rostock (2019)
30. Lienert, T., Siewert, T., Babu, S., Acoff, V.: Hybrid laser arc welding. *Weld. Fundam Processes*. **6**, 321–328 (2011)
31. Bunaziv, I., et al.: Hybrid welding possibilities of thick sections for arctic applications. *Phys. Procedia*. **78**, 74–83 (2015)
32. Wahba, M., Mizutani, M., Katayama, S.: Single pass hybrid laser-arc welding of 25mm thick square groove butt joints. *Mater. Design*. **97**, 1–6 (2016)
33. Gook, S., Gumenyuk, A., Rethmeier, M.: Hybrid laser arc welding of X80 and X120 steel grade. *Sci. Technol. Weld. Joining*. **19**(1), 15–24 (2014)
34. Üstündağ, Â., Gook, S., Gumenyuk, A., Rethmeier, M.: Mechanical properties of single-pass hybrid laser arc welded 25 mm thick-walled structures made of fine-grained structural steel. *Procedia Manuf.* **36**, 112–120 (2019)
35. Üstündağ, Â., Avilov, V., Gumenyuk, A., Rethmeier, M.: Full penetration hybrid laser arc welding of up to 28 mm thick S355 plates using electromagnetic weld pool support. In *J. Phys. Conf. Ser* (Vol. 1109, No. 1). (2018), November
36. Bunaziv, I., Akselsen, O.M., Frostevarg, J., Kaplan, A.F.: Deep penetration fiber laser-arc hybrid welding of thick HSLA steel. *J. Mater. Process. Technol.* **256**, 216–228 (2018)
37. Wu, Y., Cai, Y., Sun, D., Zhu, J., Wu, Y.: Microstructure and properties of high-power laser welding of SUS304 to SA553 for cryogenic applications. *J. Mater. Process. Technol.* **225**, 56–66 (2015)
38. Xin, D., Cai, Y., Hua, X.: Effect of preheating on microstructure and low-temperature toughness for coarse-grained heat-affected zone of 5% ni steel joint made by laser welding. *Weld. World*. **63**(5), 1229–1241 (2019)
39. Kim, J., Kim, J.: Laser welding of ASTM A553-1 (9% Nickel Steel) (PART II: Comparison of Mechanical properties with FCAW). *Metals*. **10**(8), 999 (2020)
40. El-Batahgy, A.M., Gumenyuk, A., Gook, S., Rethmeier, M.: Comparison between GTA and laser beam welding of 9% ni steel for critical cryogenic applications. *J. Mater. Process. Technol.* **261**, 193–201 (2018)
41. El-Batahgy, A., Gook, S., Gumenyuk, A., Rethmeier, M.: Effect of laser-beam and hybrid-laser-arc welding parameters and filler metal on microstructure and mechanical properties of thick heat-treated steel X8Ni9 + QT640 for cryogenic service. 4th International Conference on Welding and Failure Analysis of Engineering Materials. Aswan, Egypt (2018)
42. Gook, S., Krieger, S., Gumenyuk, A., El-Batahgy, A.M., Rethmeier, M.: Notch impact toughness of laser beam welded thick sheets of cryogenic nickel alloyed steel X8Ni9. *Procedia CIRP*. **94**, 627–631 (2020)
43. Karhu, M., Kujanpää, V., Gumenyuk, A., Lammers, M.: Study of Filler Metal Mixing and its Implication on Weld Homogeneity of Laser-Hybrid and Laser Cold-Wire Welded Thick Austenitic Stainless Steel Joints, 32nd Int. Congress on Lasers and Electro-Optics (ICALEO2013), Oct. 6–10, 2013, Miami, FL, U.S.A., Paper ID: 906, pp. 252–261
44. Zhao, L., et al.: Influence of Welding parameters on distribution of feeding elements in CO₂ laser GMA hybrid welding. *Sci. Technol. Weld. Joining*. **14**(5), 457–467 (2009)
45. Bunaziv, I., Wenner, S., Ren, X., Frostevarg, J., Kaplan, A.F., Akselsen, O.M.: Filler metal distribution and processing stability in laser-arc hybrid welding of thick HSLA steel. *J. Manuf. Process.* **54**, 228–239 (2020)
46. Sato, Y., Sugisawa, K., Aoki, D., Yamamura, T.: Viscosities of Fe–Ni, Fe–Co and Ni–Co binary melts. *Meas. Sci. Technol.* **16**(2), 363 (2005)
47. Kawahito, Y., Matsumoto, N., Abe, Y., Katayama, S.: Relationship of laser absorption to keyhole behavior in high power fiber laser welding of stainless steel and aluminum alloy. *J. Mater. Process. Technol.* **211**(10), 1563–1568 (2011)
48. Meng, X., Putra, S.N., Bachmann, M., Artinov, A., Rethmeier, M.: Influence of the free surface reconstruction on the spatial laser energy distribution in high power laser beam welding modeling. *J. Laser Appl.* **34**(4), 042023 (2022)
49. Kinney, C.C., Pytlewski, K.R., Khachatryan, A.G., Morris, J.W. Jr.: The microstructure of lath martensite in quenched 9Ni steel. *Acta Mater.* **69**, 372–385 (2014)

50. Jahrsengene, G., Wenn, M., Karlsen, M., Westermann, I., Akselsen, O.M., Hjelen, J.: EBSD quantification of retained austenite in 9% Ni steel related to thermal treatments. In The Twenty-fifth International Ocean and Polar Engineering Conference. OnePetro. (2015), June
51. Maurer, W., Ernst, W., Rauch, R., Vallant, R., Enzinger, N.: Einfluss Der Weichen Zone auf die Mechanischen Eigenschaften Hochfester Schweißverbindungen, pp. 10–15. Schweiss-& Prüftechnik (2013)
52. Muhammad, S., Miikka, K., Suck-Joo, N., Sang-Woo, H., Veli, K.: Effect of leading and trailing torch configuration on mixing and fluid behavior of laser-gas metal arc hybrid welding. J. Laser Appl. **29**(4), 042009 (2017)
53. Rethmeier, M., Gook, S., Lammers, M., Gumenyuk, A.: Laser-hybrid welding of thick plates up to 32 mm using a 20 kW fibre laser. Q. J. Japan Weld. Soc. **27**(2), 74s–79s (2009)
54. Westin, E.M., Stelling, K., Gumenyuk, A.: Single-pass laser-GMA hybrid welding of 13.5 mm thick duplex stainless steel. Weld. World. **55**(1–2), 39–49 (2011)
55. Xu, T., Shi, Y., Jiang, Z., Wu, L., Ma, Y., Wang, Z.: Improvement of cryogenic toughness for 9% ni steel keyhole TIG butt-welded joints with a ni interlayer. Mater. Sci. Engineering: A. **835**, 142661 (2022)
56. Straße, A., Üstündağ, A., Gumenyuk, A., Rethmeier, M.: LMD coatings as filler material for laser beam welded 30 mm thick plates. Procedia CIRP. **94**, 293–297 (2020)
57. Hilkes, J., Neessen, F.: Welding 9% nickel steel for liquefied natural gas (LNG) applications. Weld. Cut. **2**, 103 (2007)

Publisher's Note Springer Nature remains neutral with regard to jurisdictional claims in published maps and institutional affiliations.

Authors and Affiliations

Sergej Gook¹ · Abdel-Monem El-Batahgy² · Andrey Gumenyuk³ · Max Biegler¹ · Michael Rethmeier^{1,3,4}

✉ Sergej Gook
sergej.gook@ipk.fraunhofer.de

Abdel-Monem El-Batahgy
elbatahgy@yahoo.com

Andrey Gumenyuk
andrey.gumenyuk@bam.de

Max Biegler
max.biegler@ipk.fraunhofer.de

Michael Rethmeier
michael.rethmeier@bam.de

¹ Joining and Coating Technology, Fraunhofer Institute for Production Systems and Design Technology IPK, Pascalstrasse 8-9, Berlin 10587, Germany

² Manufacturing Technology Department, Central Metallurgical R&D Institute (CMRDI), P. O.Box: 87, Helwan, El-Tabbin, Cairo, Egypt

³ Bundesanstalt für Materialforschung und –prüfung (BAM), Unter den Eichen 87, Berlin 12205, Germany

⁴ Institute of Machine Tools and Factory Management, Technische Universität Berlin, Pascalstraße 8-9, Berlin 10587, Germany